Seeing With Sound - A Trans-Atlantic Study of the Mesopelagic Community

Brita Bøckmann

Master of Science Thesis

Section for Aquatic Biology and Toxicology
Department of Biosciences
Faculty of Mathematics and Natural Sciences

Autumn 2021

Seeing With Sound – A Trans-Atlantic Study of the Mesopelagic Community

© Brita Bøckmann

2021

Seeing with Sound – A Trans-Atlantic Study of the Mesopelagic Community

Brita Bøckmann

http://www.duo.uio.no

Print: Reprosentralen, Universitetet i Oslo

Acknowledgement

I would like to thank my supervisors, Stein Kaartvedt and Josefin Titelman, Svenja Christiansen, and Hilde Nikolaisen and Thor Klevjer for all the valuable insights they've given me. This has been an amazing project to work on, and I have truly enjoyed myself.

I would like to thank my family, Anders and Theodor, for the kindness and patience they've shown me throughout this process. I could not have done this without them.

Lastly, I would like to thank my mother and siblings who always encourage me, and who makes me think I can do anything in the whole wide world.

Abstract

The mesopelagic layers and its inhabitants are still uncharted territory. Large discrepancies in recent biomass estimates encourage a better understanding of this important ecosystem. One of the most prominent features of the mesopelagic is the daily migrations taking place between the mesopelagic zone and the sunlit euphotic zone (DVM), which enables foraging near the ocean surface during night-time when low-light conditions may serve as protection against visual predation. DVM by mesopelagic organisms constitutes the largest migrations event in the world, and it follows that DVM plays and essential role in transporting carbon from the euphotic zone towards the deep ocean. Mesopelagic micronekton form acoustic deep scattering layers, governed hydrographic features such as oxygen, fluorescence, temperature and light.

In this thesis, I used multi-frequency acoustic backscatter (s_A) recorded at 18 and 38 kHz (proxy for biomass) and environmental data (CTD measurements) collected during a scientific cruise with the Norwegian research vessel "Kronprins Haakon". The study took place across the Atlantic Ocean between 1th of December 2018 and the 9th of January 2019. The data was used to study the vertical (DVM) and latitudinal distributional patterns of mesopelagic organisms across the Atlantic Ocean. I also studied how daytime scattering layers (daytime WMDs) and migrating proportions (MPs) related to light, oxygen, temperature and fluorescence in the study region.

The results show that vertical and latitudinal distributions of acoustic backscatter (s_A), daytime scattering layers (daytime WMDs) and migrating proportions (MPs) varies between frequencies (18 and 38 kHz) and regions (NE Atlantic, Cape Verde front, equatorial region, Brazilian shelf, and the Brazil-Malvinas Confluence). The acoustic variability observed between frequencies show that migrating scattering layers are more prominent at the 18 kHz frequency, while non-migrating deep layers are more prominent the 38 kHz frequency. The regional distributions show that the depth at which daytime deep scattering layers occur (daytime WMDs) are associated with oxygen and irradiance, while the proportions of the mesopelagic community exhibiting DVM behaviour (MPs) are governed by oxygen, fluorescence and irradiance. The results also show that different environmental parameters are important at different frequencies.

Table of contents

1 Introduction

The mesopelagic zone, or the 'twilight zone', is an oceanic layer that ranges between 200 and 1000 m below the sea surface. Limited by light, this environment is characterized by the absence of photosynthesis, the ground stone for most trophic food chains. However, adaptations to low-light conditions such as sensitive eyes and bioluminescent organs, allow for predation, predator-avoidance and mating by mesopelagic organisms (Warrant & Locket, 2004). Micronekton (~2–20 cm in length) inhabiting the mesopelagic, consist mainly of small fish, squid, gelatinous organisms and crustaceans (Rudy J Kloser, Ryan, Young, & Lewis, 2009). The mesopelagic fishes of the family Myctophidae and the genus Cyclothone. likely dominate the mesopelagic community (Irigoien et al., 2014; Rudy J Kloser et al., 2009; Olivar et al., 2017).

A prominent feature of the mesopelagic is the daily migrations taking place between the mesopelagic zone and the sunlit euphotic zone (D. Bianchi & Mislan, 2016). Diel vertical migration (DVM) behaviour of zooplankton and micronekton enables foraging near the ocean surface during night-time, in which the low-light conditions may serve as protection against visual predation (Hays, 2003; Rosland & Giske, 1994). The proportion of the mesopelagic community performing DVM may vary throughout the world oceans (T. A. Klevjer et al., 2016), within populations (Kaartvedt, Titelman, Røstad, & Klevjer, 2011) and species (Pearre, 2003), and between seasons (Staby & Aksnes, 2011). DVM behaviour plays a key role in the contribution to the vertical carbon flux, in which carbon is actively transported from the euphotic zone, where carbon is ingested, to the mesopelagic zone, where carbon is released through respiration, excretion and mortality (Bollens, Rollwagen-Bollens, Quenette, & Bochdansky, 2010; PC Davison, Checkley Jr, Koslow, & Barlow, 2013; Irigoien et al., 2014; Thor Aleksander Klevjer et al., 2016). A study found that the active transport of carbon mediated by mesopelagic fishes ranged between ~10-40% of the total carbon export in the northeast Pacific Ocean (PC Davison et al., 2013). Increased knowledge on the vertical migration patterns of mesopelagic fish may therefore contribute to our understanding of the global carbon cycle and food web interactions.

Mesopelagic micronekton form acoustic deep scattering layers (DSLs) that can be observed throughout the world ocean, although distributional patterns may vary across and within ocean

boundaries (Aksnes et al., 2017; Irigoien et al., 2014; Thor Aleksander Klevjer et al., 2016). Variations in daytime DSLs have been explored together with environmental parameter such as oxygen, temperature and fluorescence (Thor Aleksander Klevjer et al., 2016), density (Cade & Benoit-Bird, 2015), and sunlight (Aksnes et al., 2017). Shallow daytime DSLs have been associated with oxygen-depleted waters (Daniele Bianchi, Galbraith, Carozza, Mislan, & Stock, 2013; Netburn & Koslow, 2015), in which avoidance of hypoxia have been hypothesized to cause variations in daytime DSLs (Gilly, Beman, Litvin, & Robison, 2013; Koslow, Goericke, Lara-Lopez, & Watson, 2011). However, recent studies have found daytime DSLs deep into anoxic layers, indicating that hypoxia avoidance can't be the main driver for shallow daytime DSLs in low-oxygen regimes (Irigoien et al., 2014; Thor Aleksander Klevjer et al., 2016). A study by Aksnes et al. (2017) found that the global variations in daytime DSLs could be attributed to variations in light penetration.

Acoustic methods have traditionally been applied to the assessment of fish stocks, and has been deemed a useful method by the scientific community in studying abundance (Irigoien et al., 2014; Koslow, Kloser, & Williams, 1997), vertical distribution (Godø, Patel, & Pedersen, 2009; Klevjer et al., 2020), horizontal distribution (Escobar-Flores, O'Driscoll, & Montgomery, 2018), and behaviour (Christiansen, Klevjer, Røstad, Aksnes, & Kaartvedt, 2021) in mesopelagic communities. Acoustic instruments such as echosounders, transmit and receives soundwaves that travel long distances in water, which allows for the detection of micronekton on large spatial and temporal scales. Most fishing and research vessels are equipped with echosounders, making acoustic data readily available to the scientific community. The amount of sound that is scattered by individual micronekton (i.e. acoustic backscatter), vary with size, depth and density (P. C. Davison, Koslow, & Kloser, 2015). The density of mesopelagic fish is especially affected by the presence of a gas-filled swimbladders, which increases their target strength (P. C. Davison et al., 2015). Acoustic backscatter may be recorded on multiple frequencies, including standard frequencies of 18, 38, 70, 120 and 200 kHz. The selection criteria for which frequency to utilize, is based on depth penetration, resonance and body size (P. C. Davison et al., 2015). When studying mesopelagic micronekton, lower frequencies (18 and 38 kHz) is preferred giving the depth range of mesopelagic scattering layers and size distributions (P. C. Davison et al., 2015; Pena, Cabrera-Gamez, & Dominguez-Brito, 2020).

The mesopelagic zone is still one of the most unexplored territories on the planet, along with its inhabitants. Biomass estimates varies greatly, ranging between 1 gigaton (Gt) using trawl methods (Gjøsæter & Kawaguchi, 1980), and ~11-15 Gt using acoustic estimation methods (Irigoien et al., 2014). This suggest that there may be a substantial amount of fish biomass in the mesopelagic, which has led to increased commercial interest in this potentially unexploited resource (St. John et al., 2016). However, the benefits of exploiting this resource (food production, nutraceutical products) is off-set by the potential ecosystem services the mesopelagic community provides (carbon sequestration, maintaining biodiversity) (St. John et al., 2016). By filling in the knowledge gap about the abundance and spatial distribution of the mesopelagic community, as well as the environmental conditions that might drive these processes, we are better apt to develop ecosystem models which will aid in the assessment of ecosystem status, impacts of climate change and resource-exploitation (Handegard et al., 2013; Lehodey, Murtugudde, & Senina, 2010).

1.1 Aims

In this thesis, I use multi-frequency acoustic backscatter (s_A) recorded at 18 and 38 kHz (proxy for biomass) to study the vertical and latitudinal distributional patterns of mesopelagic organisms across the Atlantic Ocean. This gives me an unique opportunity to study diel vertical migration behaviour, deep daytime scattering layers and migrating proportions in different regions, characterized by varying hydrographic features. I also study daytime scattering layers and migrating proportions in relation to light, oxygen, temperature and fluorescence.

2 Methods

2.1 Study region

The data was collected during a scientific cruise (no. 2019716) with the Norwegian research vessel "Kronprins Haakon". The study took place across the Atlantic Ocean, departing from Norway on the 1th of December 2018, and arriving in Chile on the 9th of January 2019. The study region was interesting to investigate due to its varying hydrographic properties and productivity gradients, as well as the major current systems and upwelling regions along the cruise track.

The Azores Current (AC) which is part of the North Atlantic subtropical gyre, flows in a southeastward direction, crossing the Mid Atlantic Ridge (34°N, 37°W) (Kase, Zenk, Sanford, & Hiller, 1985), before turning southwards, feeding into the Canary Current (New, Jia, Coulibaly, & Dengg, 2001) and the North Equatorial Current (NEC) (Maillard & Kase, 1989). The westward flowing North and South Equatorial Currents (NEC and SEC) and the eastward flowing North Equatorial Countercurrent (NECC), are surface currents driven by diverging westward trade winds in the Northern and Southern Hemispheres, ultimately causing upwelling at the equator (Stramma, Steele, Thorpe, & Turekian, 2001). The South Equatorial Current (SEC) feeds into the southward flowing Brazil Current (BC), which transport warm water along the east coast of South America (A. A. Bianchi, Giulivi, & Piola, 1993). The western region of the tropical Atlantic, along the continental slope of Brazil, is characterized as one of the most nutrient-poor (oligotrophic) zones in the world (Morel, Claustre, & Gentili, 2010). North of the Falkland Islands (38°S), the southward warm Brazil Current meets the cold northward Malvinas (Falkland) current, a branch of the Arctic Circumpolar Current (ACC) (A. A. Bianchi et al., 1993). The merging of these two currents results in a highly energetic region, called the Brazil-Malvinas Confluence (Gordon, 1989). This region is characterized by vigorous mixing of water masses with different hydrographic properties, causing a thermohaline front (A. A. Bianchi et al., 1993).

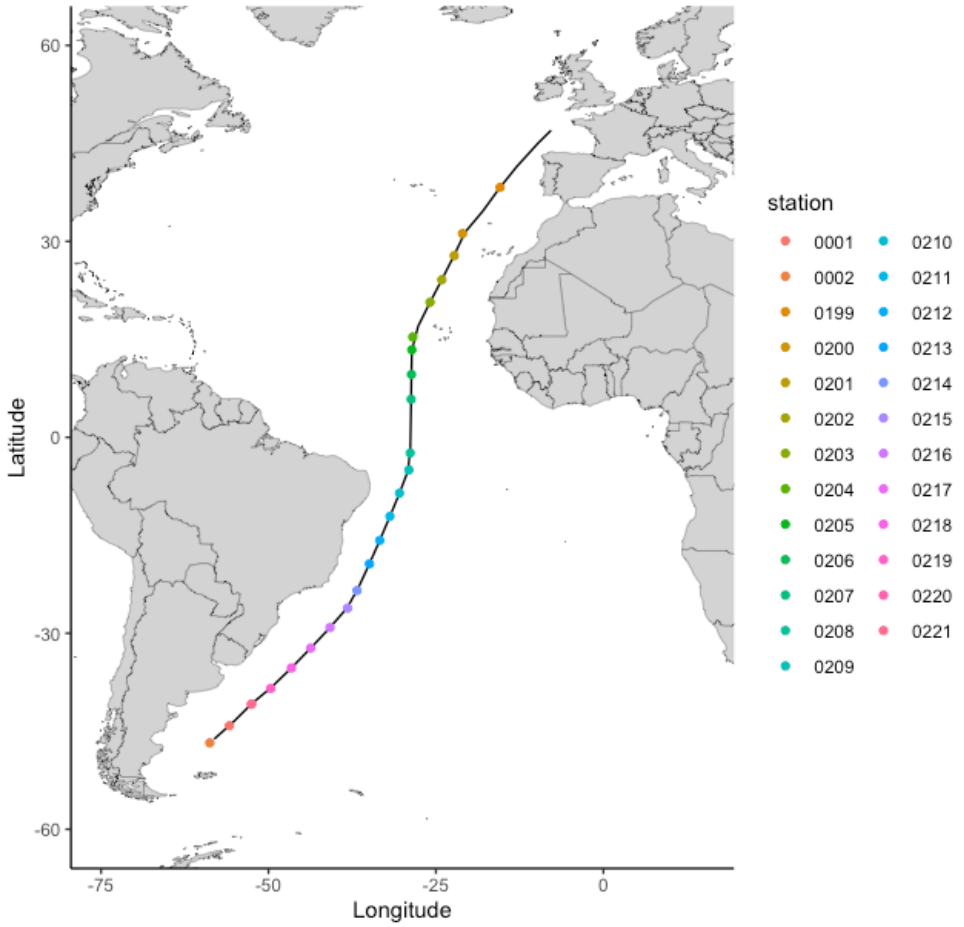

Fig. 2.1: Cruise track. The cruise track (black line) marked with CTD stations (dots).

2.2 Environmental data

2.2.1 CTD data

Temperature (°C), salinity (PSU), dissolved oxygen (ml liter^{-1}), fluorescence (relative units) and irradiance (µmol photons/m^2/sec), were measured for each meter with a CTD instrument (Sea-Bird SBE 9). The CTD was cast 25 times during the cruise, including 21 casts between ~0-300 m, and 4 casts between ~0-1500 m. The number of CTD casts that could be lowered to 1500 m were limited due to time constraints.

The CTD files were imported to RStudio for further analysis, using the function 'oce::read.ctd'. Temperature, salinity, oxygen and fluorescence were interpolated using the functions 'akima::interp' and 'akima::interp2xyz' in RStudio, for the purpose of estimating

environmental values in between CTD stations and at depths deeper than the available measurements from the CTD. I chose an interpolation method instead of an extrapolation method, because I was interested in estimating unknown values that fell between my known values, i.e. in between each CTD station. The 4 CTD stations that contained data between ~0-1500 m made it possible to estimate unknown values in the mesopelagic zone (200-1000 m).

The Akima interpolation method implements bivariate interpolation on to a grid, designed for irregularly spaced input data. I found this interpolation method appropriate due to the CTD stations being unevenly spaced along the cruise track. After interpolating the data horizontally (between CTD stations) and vertically (5-1000 m), the data was visualized by using the function 'ggplot2::ggplot' in RStudio.

Estimation of irradiance at depths deeper than the available irradiance measurements from the CTD was not possible using the Akima interpolation method in RStudio. Irradiance measurements that dropped below detectable levels (0,06 µmol photons/m^2/sec) were treated as missing values. This resulted in a max. depth between 129-263 m for each CTD station, which made interpolation of irradiance at greater depths impossible.

The relationship between irradiance and depth (m) was assessed by performing a Pearson correlation test (ρ = -0.90, $p < 0.001$), using the function 'cor.test' in Rstudio. Below the deepest available irradiance measurements (>129-263 m), I assumed a constant relationship between irradiance and depth (m) by performing a simple linear regression analysis $\log_{10}$irradiance ~ depth (m) for each CTD station (R^2 = 0.955-0.997, $p < 0.01$, n = 23). Two stations were excluded from the analysis due to missing data (#0199 and #0204). My assumption of a constant relationship between irradiance and depth below the deepest available irradiance measurements, fails to include the change of light quality with increasing depth, in which longer wavelengths attenuates more rapidly in upper surface layers while shorter wavelengths penetrates deeper (Penta et al., 2008). On the positive side, by combining the observed irradiance measurements (from the sea surface to max. depth of observed irradiance) with the estimated irradiance values (from max. depth to 1000 m), I do not assume a constant relationship between irradiance and depth for the whole water column. This is important due to the possible effects of light attenuation caused by phytoplankton absorption in the upper water column (Penta et al., 2008).

The combined observed and estimated values of irradiance was used in the stepwise multiple regression models of migratory proportions (MP) and daytime weighted mean depths (WMDs).

2.3 Acoustic data

The acoustic data was recorded continuously on multiple frequencies (18, 38 and 70kHz) using a Simrad EK80 calibrated split-beam echosounder with beam widths of 7° (38 kHz) and 11° (18 kHz), and a ping rate of 1 transmitted pulse per 4 s. Acoustic data recorded at 18 and 38 kHz was used for further analysis. The nautical area scattering coefficient [NASC; s_A (m^2 nautical $mile^{-2}$)] was used as the measurement for the acoustic backscatter, and as proxy for biomass in the thesis.

The echosunder transmits sound pulses with distinct frequencies into the water column and measures the return echo. The return echo, or target strength (TS; measured in db), of the organism under study, varies with size, body density and depth (Davison et al., 2015). TS have been found to linearly increase with size, however, decreasing body density, swimbladder resonance, and ontogenetic changes in swimbladder inflation have all been found to affect the relationship between TS and body size in mesopelagic fishes (P. C. Davison et al., 2015). The presence of a gas-filled, lipid-filled or reduced swimbladder, contributes to the density of an individual fish and consequently increase the backscatter from the fish body (P. Davison, 2011; P. C. Davison et al., 2015). Swimbladder morphology may also vary between species within the same genus. Some species of bristlemouths (Cyclothone) have gas-filled swimbladders, some lack gas-filled swimbladders, and some species only have gas-filled swimbladders in juvenile life-stages (P. Davison, 2011). To further complicate the matter, swimbladder resonance increase with depth (P. C. Davison et al., 2015), and so resonance in swimbladdered fish may change during DVM (Godø et al., 2009). Swimbladder resonance may result in positively biased estimates of fish abundance, as resonance from one individual fish may contribute as much to the scattering strength as one hundred non-resonant fish (Gjøsæter & Kawaguchi, 1980).

The considerations involved in selecting a frequency suitable for the environment under study, include absorption (i.e. depth penetration), resonance, and body size of the organisms present (P. C. Davison et al., 2015). Higher frequencies (≥120 kHz) are not able to reach the daytime depths of mesopelagic micronekton, and the 70 kHz frequency produce scatter from non-target zooplankton (P. C. Davison et al., 2015). The disadvantages of using lower frequencies (18 and 38 kHz) include swimbladder resonance from mesopelagic fishes and the exclusion of fish without swimbladders (P. C. Davison et al., 2015). Davison et al. (2015) argues that 18 kHz poorer choice when studying mesopelagic fishes, seeing as a larger proportion of mesopelagic fish resonate at 18 kHz compared with 38 kHz. However, the use of multi-frequency may provide information about the species composition of acoustic scattering layers (Godø et al., 2009; R. Kloser, Ryan, Sakov, Williams, & Koslow, 2002; Pena et al., 2020). The 18 kHz frequency is especially suitable for detection of migratory scattering layers (i.e. mesopelagic fishes exhibiting DVM behaviour), due to changes in swimbladder resonance as the fishes move vertically in the water column (Godø et al., 2009). Mesopelagic fishes exhibiting DVM behaviour may therefore scatter more at 18 kHz during night-time when feeding in upper layers, and less during daytime when occupying deeper layers (Godo, Patel, & Pedersen, 2009).

2.3.1 Post-processing in LSSS

The acoustic data was processed and interpreted in the Large Scale Survey System (LSSS), in which it was integrated in 2-minute-by-10-metre bins at a threshold of -90 dB. The raw files contained noise spikes and background noise which was removed by Thor Klevjer from the Institute of Marine Research, using KORONA filters implemented in the LSSS software. The data was also subjected to manual scrutiny to remove remaining noise, such as additional noise spikes, false bottoms and sea mounts. Removing noise from the data runs the risk of removing acoustic backscatter that is associated with the environment of study. However, failing to do so would result in overrepresentation of acoustic backscatter. The noise removal had to be performed separately for 18 and 38 kHz, seeing as the frequencies differ in their sensitivity to noise. The acoustic backscatter was divided into 4 categories in the LSSS software: pelagic s_A (10-200 m), mesopelagic s_A (200-1000 m), bathypelagic s_A (1000-1500 m) and total s_A (10-1500 m). The first 10 meters of the water column was not included in the analysis, due to noise

at the sea surface. Finally, the data was exported by generating two reports, one for each frequency, using format 16. The data was imported to RStudio for further analysis.

2.3.2 Data analysis in RStudio

2.2.3 Vertical patterns

Acoustic backscatter (s_A) recorded at 18 and 38 kHz was classified as either 'day' or 'night' by estimating sunrise and sunset times at the mean latitude and longitude for each day of the survey. The sunrise and sunset times were estimated by using the 'maptools::sunriset' function in RStudio. The crepuscular periods (1 hour before and after sunrise and sunset), in which the mesopelagic community ascend and descend in association with DVM, were excluded in the analysis. Data with a time stamp between sunrise and sunset was categorized as 'day' and data with a time stamp between sunset and sunrise was categorized as 'night'. To describe vertical distribution patterns and DVM behaviour, I averaged the 'day' and 'night' acoustic backscatter (s_A) for each depth bin. The mean acoustic backscatter (s_A) in the epipelagic (0-200 m) and the mesopelagic (200-1000 m), the weighted mean depths (WMDs) and the migration proportions (MP) were calculated from these data. The acoustic backscatter recorded on the last day of the survey was not a complete day, and so this was excluded from the analysis.

The mean acoustic backscatter (s_A) in the epipelagic (0-200 m) and the mesopelagic (200-1000 m) was calculated by summarising the mean acoustic backscatter (s_A) for each depth bin.

Daytime WMDs was calculated using the formula:

(1) $WMD = (\Sigma (s_A D_i) / \Sigma s_{Ai})$

The migratory proportions were calculated as the ratio between mesopelagic acoustic backscatter (s_A) at day and night (3). The ratio was corrected for overall changes in total acoustic backscatter (s_A) between day and night (2):

(2) *DNR (day to night s_A ratio) = total (s_A) day / total (s_A) night.*

(3) $MP = 1 - ((s_A \text{ mesopelagic night} * DNR) / s_A \text{ mesopelagic day}), MP > 0$

To describe different vertical patterns in the study region, I selected five regions based on their hydrographic characteristics. Acoustic backscatter (s_A) recorded in the temperate North East Atlantic region (~46-36°N) was categorized as 'NE Atlantic' and consisted of 3 day/night pairs. Acoustic backscatter (s_A) recorded in the oxygen minimum layers (OMLs) of the Cape Verde frontal zone (17-11°N) was categorized as 'Cape Verde front' and consisted of 2 day/night pairs. Acoustic backscatter (s_A) recorded in the tropical equatorial region (~10°N-10°S) was categorized as 'Equatorial region' and consisted of 6 day/night pairs. Acoustic backscatter (s_A) recorded in the oligotrophic waters along the Brazilian shelf (~11.5-21°S) was categorized as 'Brazilian shelf' and consisted of 3 day/night pairs. And lastly, acoustic backscatter (s_A) recorded in the upwelling region associated with the Brazil-Malvinas Confluence (~35-42°S) was categorized as 'Brazil-Malvinas Confluence' and consisted of 3 day/night pairs.

2.2.4 Latitudinal patterns

I described the latitudinal distributional patterns at 18 and 38 kHz by averaging the mesopelagic (200-1000 m) the daytime and night-time acoustic backscatter (s_A) for each day of the transect. The data was fitted with the smoothing function 'tidyverse::geom_smooth' in RStudio.

2.4 Environmental impacts on MP and daytime WMD

Average oxygen 200-1000 m (ml l^{-1}), average fluorescence 0-200 m (relative units, a measure of chlorophyll a fluorescence), average temperature 200-1000 m (°C), and average irradiance 0-1000 m (µmol photons/m^2/sec) were checked for correlation with migratory proportion (MP) and daytime WMDs at 18 and 38 kHz, by performing Pearson's correlation tests ('GGally: ggscatmat') and stepwise multiple linear regressions 'olsrr: ols_step_both_p" in RStudio. The data used in the Pearson's correlation tests and stepwise multiple linear regressions included my own observations to the maximum depths of the CTD measurements, and the Akima interpolated values of oxygen and temperature beyond my available data.

3 Results

3.1 Environmental data

Near-surface temperature increased towards the equatorial Atlantic, in which temperatures higher than 27°C were observed at stations #0207-0210 and station #0212 (fig. 3.1). The near-surface temperature decreased towards the end of the study region, where the lowest temperature recorded (11,6°C) was observed at the final station (#0002) (fig. 3.1). Near-surface salinities higher than 37 PSU were observed in the regions adjacent to the equatorial Atlantic, at stations #0200-0202, #0212 and #0214 (fig. 3.1). Near-surface salinities were low towards the end of the study region (stations #0001-0002), in which salinities of 34 PSU were observed (fig. 3.1). Near-surface waters were always well oxygenated, although there was a tendency for higher oxygen concentrations (>6 ml l^{-1}) towards the end of the study region (stations #0001-0002) (fig. 3.1). Near-surface fluorescence showed low concentrations for the better part of the study region, although there was a tendency for higher fluorescence concentrations towards the end of the study region (station #0001) (>0 relative units) (fig. 3.1).

Vertical stratification of temperature, salinity and oxygen was apparent throughout the study region (fig. 3.1). The stratification patterns also revealed the oceanic front located at the end of the study region (fig. 3.1). There was a tendency for a shallower thermocline (~30 m) at stations #0001-0002 and a deeper thermocline at station #0202, #0212 and #0214 (fig. 3.1). The temperature gradients were higher in the equatorial region, in which the difference in temperature between the surface and 300 m could reach up to 18°C (station #0210) (fig. 3.1). The temperature gradient between 0-300 m was lower in the beginning of the study region (4°C at station #0199), and at the oceanic front towards the end of the study region (~10°C at stations #0001-0002) (fig. 3.1). The haloclines presented similar patterns to the thermoclines as there was a tendency for a deeper halocline at station #0202, #0212 and #0214 (fig. 3.1). However, subsurface layers (~45-80 m) with higher salinity concentrations were observed in the equatorial region (station #0205 and stations #0207-0208). Salinity reached a subsurface maximum (49 m) at station #0212, while the salinity concentrations at the oceanic front (stations #0001-0002) were low (~34 PSU) throughout the water column (fig. 3.1). The vertical distribution of dissolved oxygen showed a tendency for lower sub-surface (~80 m) oxygen

concentrations (<3 ml l^{-1}) at stations #0204-0211 (fig. 3.1). Oxygen concentrations less than 2 ml l^{-1} were observed from ~100-300 m at stations #0204-0205 and station #0208 (fig. 3.1). Higher concentrations of oxygen (>6 ml l^{-1}) were observed throughout the water column at the oceanic front (stations #0001-0002), in which oxygen reached a subsurface maximum (44 m) at station #0002 (fig. 3.1). The vertical distribution of fluorescence displayed higher concentration (>0 relative units) between 67 and 94 m in the equatorial region (station #0207 and #0209), and between 40 and 65 m towards the end of the study region (stations #0219-0221) (fig. 3.1). Fluorescence concentrations were conspicuously high at the oceanic front (station #0001), in which a subsurface maximum (0,5081 relative units) was observed at 35 m (fig. 3.1).

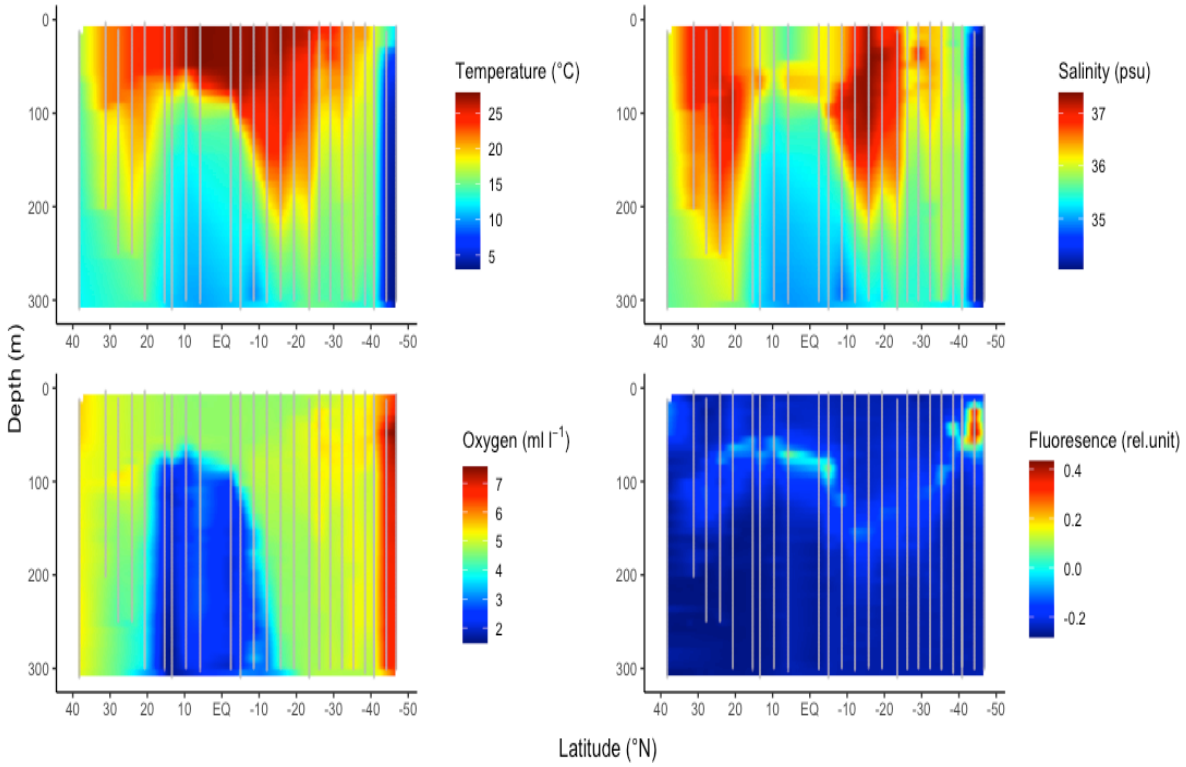

Fig. 3.1. CTD profiles. Vertical profiles (0-300 m) of temperature (°C), salinity (psu), dissolved oxygen (ml l^{-1}) and fluorescence (relative units). Grey lines represent CTD stations.

3.2 Acoustic data

3.2.1 Vertical distributions (18 and 38 kHz)

The vertical distribution of mean acoustic backscatter (s_A) recorded at 18 and 38 kHz (fig. 3.2.1) displayed varying patterns between the surface and 1000 m. However, there were some consistent patterns in the data. Day and night effects on the vertical distribution were always present, with typically higher values of acoustic backscatter (s_A) in the epipelagic (0-200 m) at night and in the mesopelagic (200-1000 m) at day (fig. 3.2.1).

The 18 kHz distribution displayed higher values of mean acoustic backscatter (s_A) in the epipelagic at night compared with the 38 kHz distribution (fig. 3.2.1). The 38 kHz distribution displayed higher values of mean acoustic backscatter (s_A) in the mesopelagic at both day and night compared with the 18 kHz distribution (fig. 3.2.1). The daytime WMD was deeper (WMD = 494 m) at the 38 kHz distribution, compared with the 18 kHz distribution (WMD = 472 m) (fig. 3.2.1, table. 3.2.1), while the migrating proportion was higher at the 18 kHz distribution (MP = 0.47) compared to the 38 kHz distribution (MP = 0.27) (fig. 3.2.1, table. 3.2.1).

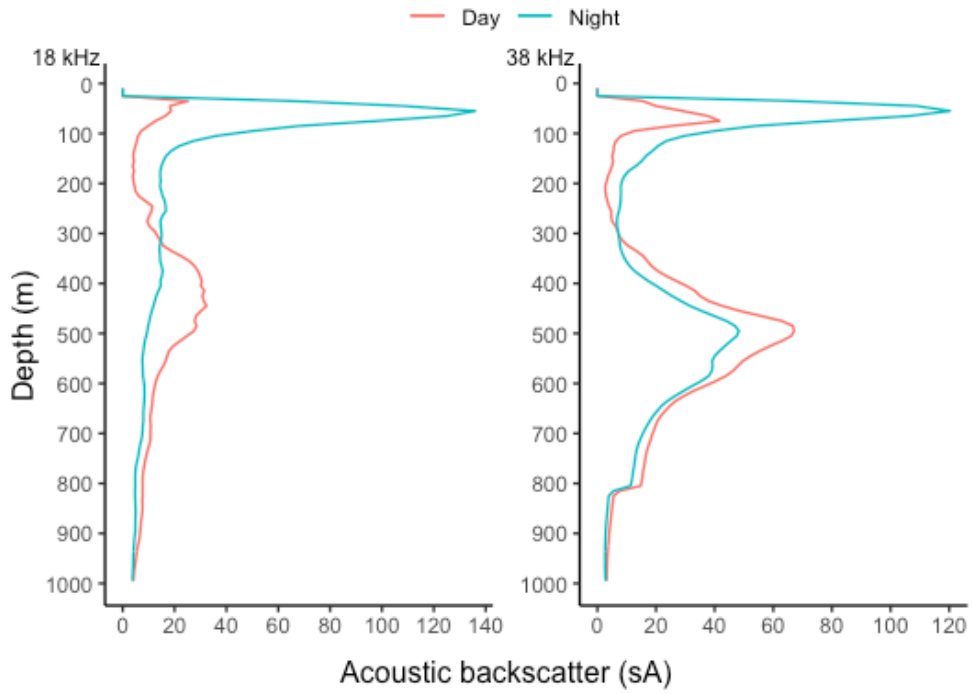

Fig. 3.2.1 Daytime and night-time vertical distribution (18 and 38 kHz). Mean acoustic backscatter (s_A) recorded on 18 kHz (A) and 38 kHz (B) (0-1000 m) at daytime (red line) and night-time (blue line), for all data.

	18 kHz	38 kHz	Units
Daytime WMD	472	494	m
Migrating proportion	0.47	0.27	
Day-night pairs	27	27	

Table 3.2.1 Daytime WMD and MP (18 and 38 kHz). Estimated parameters of daytime weighted mean depth (WMD) and migratory proportions (MP). The estimated parameters are calculated for mean acoustic backscatter (s_A) recorded at 18 kHz and 38 kHz.

3.2.2 Vertical distributions between regions (18 and 38 kHz)

The NE Atlantic region (46-36°N) displayed high variability between the vertical distributions recorded at 18 kHz (fig. 3.2.2) and 38 kHz (3.2.3). The vertical distribution recorded at 18 kHz was characterized by two distinct daytime layers at ~280 and ~380 m, a non-migratory night-time layer at ~300 m, and two night-time layers in the epipelagic (fig. 3.2.2). The proportion of migrants was 14% and the daytime WMD was 480 m (table 3.2.2). The vertical distribution recorded at 38 kHz was characterized by a deep daytime layer and a deep non-migratory night-time layer at ~550 m, and limited acoustic backscatter in the epipelagic at night (fig. 3.2.3). The migrating proportion was 2% and the daytime WMD was 586 m at the 38 kHz distribution (table 3.2.3).

The Cape Verde frontal region (17-11°N) displayed a distinctive night-time layer in the epipelagic at the 18 kHz frequency, characterized by relatively high acoustic backscatter (fig. 3.2.2). The 18 kHz distribution also displayed a daytime scattering layer at ~370 m (fig. 3.2.2). The migrating proportion was 69.4%, and the daytime WMD was 433 m (table 3.2.2). The 38 kHz distribution also displayed a distinctive night-time layer in the epipelagic and a daytime layers at approximately the same depth (~370 m) (fig. 3.2.3). The migrating proportion was 50.5 % and the daytime WMD was 449 m at the 38 kHz distribution (table 3.2.3).

The equatorial region (~10°N-10°S) displayed a distinctive night-time layer in the epipelagic, a daytime and non-migratory night-time layer at ~230 m, and a deeper daytime layer at ~380 m at the 18 kHz distribution (fig. 3.2.2). The migration proportion was 49.1% and the daytime WMD was 436 m at the 18 kHz distribution (table 3.2.2). The 38 kHz distribution also displayed a distinctive night-time layer in the epipelagic, and a daytime and non-migratory

night-time layer at ~420 m (fig. 3.2.3). The migration proportion was 40.3 % and the daytime WMD was 386 m at the 38 kHz distribution (table 3.2.3).

The Brazilian shelf region (~11.5-21°S) was characterized by a distinct night-time layer in the epipelagic, and several night-time layers between ~150-250 m at the 18 kHz distribution (fig. 3.2.2). The 18 kHz distribution also displayed several daytime-layers at ~400, ~550, ~700 and ~880 m, and non-migratory nigh-time layers at ~700 and ~880 m (fig. 3.2.2). The migration proportion was 37.3 % and the daytime WMD was 505 m at the 18 kHz distribution (table 3.2.2). The 38 kHz distribution displayed several night-time layers between the sea surface and ~250 m, two non-migratory night-time-layers at ~550 and ~800 m, and two daytime layers at approximately the same depths (fig. 3.2.3). The migration proportion was 58.9% and the daytime WMD was 490 m at the 38 kHz distribution (table 3.2.3).

The Brazil-Malvinas Confluence region (~35-42°S) displayed a distinctive night-time layer in the epipelagic and a non-migratory night-time layer at ~400 m at the 18 kHz distribution (fig. 3.2.2). The 18 kHz distribution also displayed a daytime layer at ~450 m (fig. 3.2.2). The migration proportion was 31.9 % and the daytime WMD was 478 m at the 18 kHz distribution (table 3.2.2). The 38 kHz distribution displayed a distinct daytime layer and non-migratory night-time layer at ~500 m, and a night-time layer in the epipelagic (fig. 3.2.3). The migration proportion was 10.8 % and the daytime WMD was 526 m at the 38 kHz distribution (table 3.2.3).

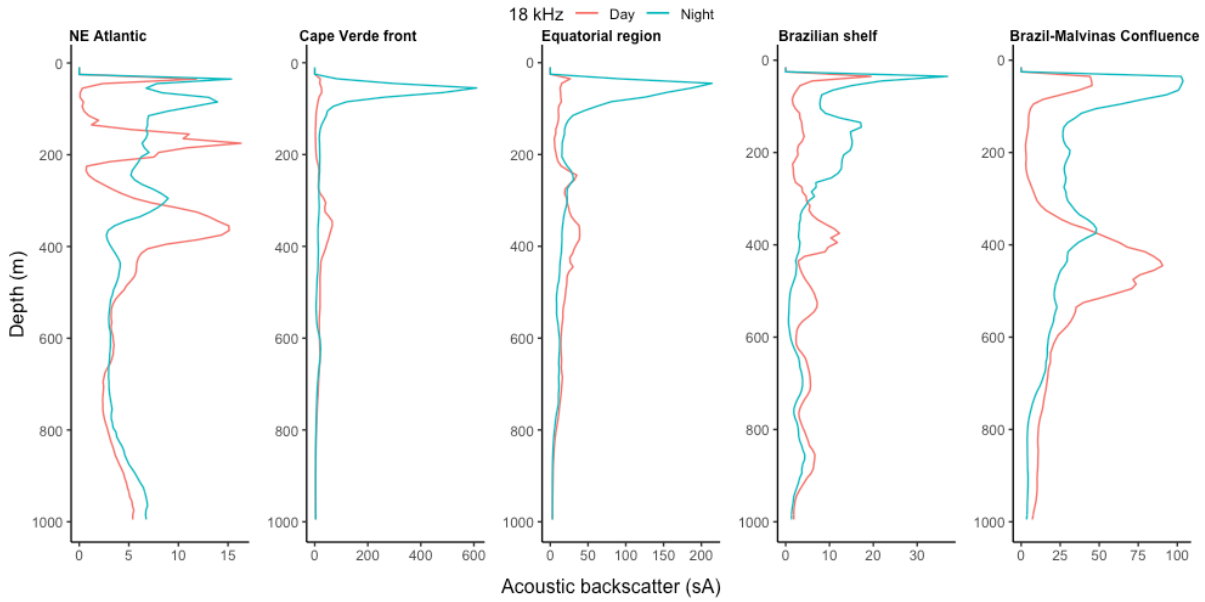

Fig. 3.2.2. Vertical distributions between regions (18 kHz). Mean acoustic backscatter (s_A) recorded at 18 kHz (0-1000 m) in the NE Atlantic (~46-36°N), the Cape Verde front (17-11°N), the Equatorial region (~10°N-10°S), the Brazilian shelf (~11.5-21°S), and the Brazil-Malvinas Confluence region (~35-42°S). The mean acoustic backscatter (s_A) was recorded at day (red line) and night (blue line).

18 kHz	NE Atlantic	Cape Verde front	Equatorial region	Brazilian shelf	Brazil-Malvinas Confluence	Units
Daytime WMD	480	433	436	505	478	m
Migrating proportion	0.140	0.694	0.491	0.373	0.319	
Day/night pairs	3	2	6	3	3	

Table 3.2.2 Daytime WMD and MP between regions (18 kHz). Estimated parameters of daytime weighted mean depth (WMD) and migratory proportions (MP) in the NE Atlantic (~46-36°N), the Cape Verde front (17-11°N), the Equatorial region (~10°N-10°S), the Brazilian shelf (~11.5-21°S), and the Brazil-Malvinas Confluence region (~35-42°S).
The estimated parameters are calculated for mean acoustic backscatter (s_A) recorded at 18 kHz.

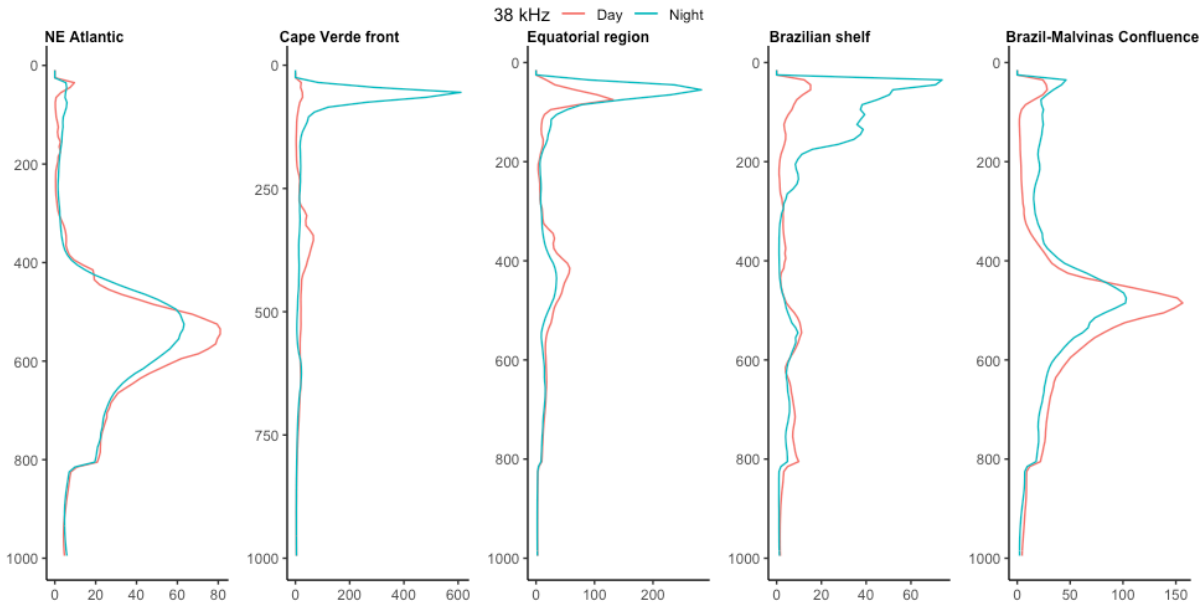

Fig. 3.2.3. Vertical distributions between regions (38 kHz). Mean acoustic backscatter (s_A) recorded at 38 kHz (0-1000 m) in the NE Atlantic (~46-36°N), the Cape Verde front (17-11°N), the Equatorial region (~10°N-10°S), the Brazilian shelf (~11.5-21°S), and the Brazil-Malvinas Confluence region (~35-42°S). The mean acoustic backscatter (s_A) was recorded at day (red line) and night (blue line).

38 kHz	NE Atlantic	Cape Verde front	Equatorial region	Brazilian shelf	Brazil-Malvinas Confluence	Units
Daytime WMD	586	449	386	490	526	m
Migrating proportion	0.02	0.505	0.403	0.589	0.108	
Day/night pairs	3	2	6	3	3	

Table 3.2.3 Daytime WMD and MP between regions (38 kHz). Estimated parameters of daytime weighted mean depth (WMD) and migratory proportions (MP) in the NE Atlantic (~46-36°N), the Cape Verde front (17-11°N), the Equatorial region (~10°N-10°S), the Brazilian shelf (~11.5-21°S), and the Brazil-Malvinas Confluence region (~35-42°S).
The estimated parameters are calculated for mean acoustic backscatter (s_A) recorded at 38 kHz.

3.3 Latitudinal distribution

The latitudinal distribution of mean acoustic backscatter (s_A) recorded at 18 and 38 kHz (fig. 3.3) displayed similar patterns in the equatorial region (~10°N-10°S) and in the Brazilian shelf region (~11.5-21°S), while high variability between frequencies was observed between the North East Atlantic region and the equatorial region (~46-10°N), and in the Brazil-Malvinas Confluence region (~35-42°S).

For the 18 kHz distribution, mean acoustic backscatter (s_A) increased between the North East Atlantic region and the equatorial region (~46-5°N), followed by a decrease towards the Brazilian shelf region (~5°N-21°S). The mean acoustic backscatter (s_A) increased between the Brazilian shelf region towards the Brazil-Malvinas Confluence region (~21-42°S), before decreasing towards the end of the study region (42-48°S).

For the 38 kHz distribution, mean acoustic backscatter (s_A) increased in the North East Atlantic region (~46-36°N), followed by a decrease towards the Brazilian shelf region (~36°N-21°S). From the Brazilian shelf region, mean acoustic backscatter (s_A) increased towards the Brazil-Malvinas Confluence region (~21-42°S), before decreasing towards the end of the study region (42-48°S).

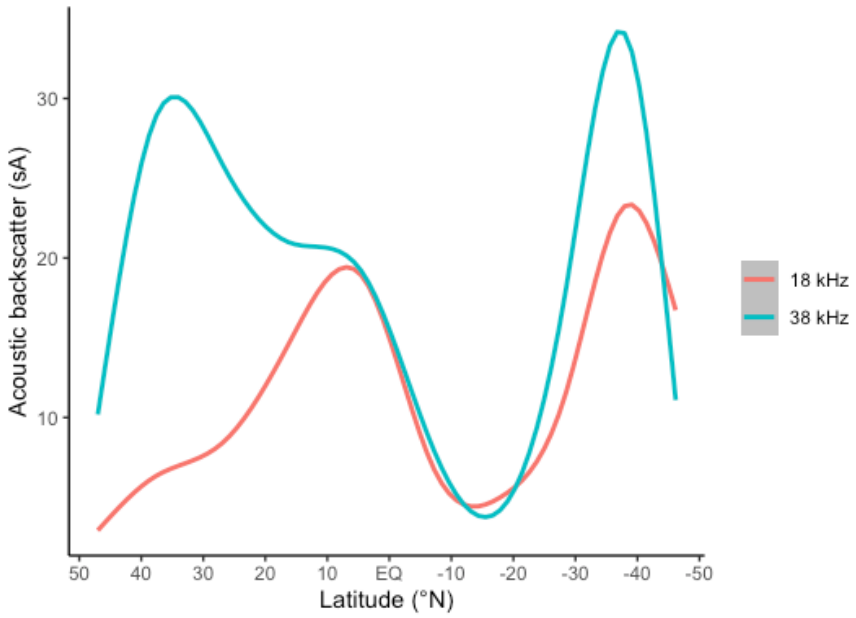

Fig 3.3. Latitudinal distribution (18 and 38 kHz). Mean acoustic backscatter (s_A) recorded at 18 and 38 kHz in the mesopelagic zone (200-1000 m).

3.4 Environmental influences on migrating proportions

Environmental variables (oxygen, fluorescence, temperature and irradiance) were checked for correlation with migrating proportions (MP) at 18 kHz and 38 kHz, using Pearson's correlation tests (fig. 3.4.2 and 3.4.4) and stepwise multiple linear regressions (fig. 3.4.1 and 3.4.3). I used average oxygen 200-1000 m (ml l^{-1}), average fluorescence 0-200 m (relative units, a measure of chlorophyll a fluorescence), average temperature 200-1000 m (°C), and average irradiance 0-1000 m (µmol photons/m^2/sec).

3.4.1 Stepwise multiple linear regression MP (18 kHz)

Average oxygen had the strongest correlation with MP at 18 kHz (ρ = -0.59), followed by average fluorescence (ρ = -0.55), average temperature (ρ = 0.41) and average irradiance (ρ = 0.14) (fig. 3.4.2).

Average oxygen (200-1000 m) and average fluorescence (0-200 m) appeared to explain 42.0% of the variation in MP at 18 kHz (adj. R^2 = 0.420). MP appeared to increase with decreasing oxygen and decreasing fluorescence (MP = -0.051*(avg. oxygen) -1.603*(avg. fluorescence), n = 24, $p < 0.05$) (fig. 3.4.1).

COEFFICIENTS	ESTIMATE	STD.ERROR	T-VALUE	P-VALUE
INTERCEPT	0.334	0.188	1.774	0.091
AVG. OXYGEN	-0.051	0.020	-2.568	0.018
AVG. FLUORESCENCE	-1.603	0.715	-2.243	0.036

Fig. 3.4.1 Stepwise multiple linear regression MP (38 kHz).

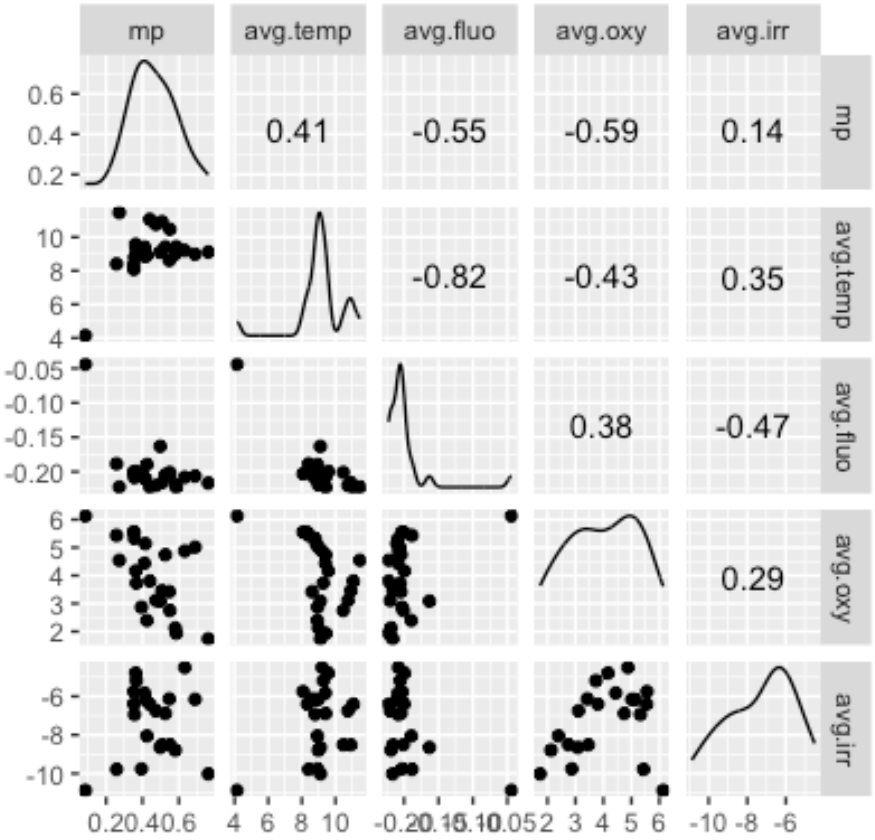

Fig 3.4.2. Correlation matrix MP (18 kHz). Pearson's correlation coefficients between migrating proportions (mp), average oxygen 200-1000 m (avg.oxy), average fluorescence 0-200 m (avg.fluo), average temperature 200-1000 m (avg.temp), and average irradiance 0-1000 m (avg.irr) at 18 kHz.

3.4.2 Stepwise multiple linear regression MP (38 kHz)

Average oxygen had the strongest correlation with MP at 38 kHz (ρ = -0.43), followed by average irradiance (ρ = 0.34), average fluorescence (ρ = -0.25) and average temperature (ρ = 0.11).

Average oxygen (200-1000 m) and average irradiance (0-1000 m) appeared to explain 32.7% of the variation in MP at 38 kHz (adj. R^2 = 0.327). MP appeared to increase with decreasing oxygen and increasing irradiance (MP = -0.082*(avg. oxygen) +0.052*(avg. irradiance), n = 24, $p < 0.05$).

COEFFICIENTS	ESTIMATE	STD.ERROR	T-VALUE	P-VALUE
INTERCEPT	1.049	0.207	5.056	0.000
AVG. OXYGEN	-0.082	0.028	-2.922	0.009
AVG. IRRADIANCE	0.052	0.019	2.673	0.015

Fig. 3.4.3. Stepwise multiple linear regression MP (38 kHz).

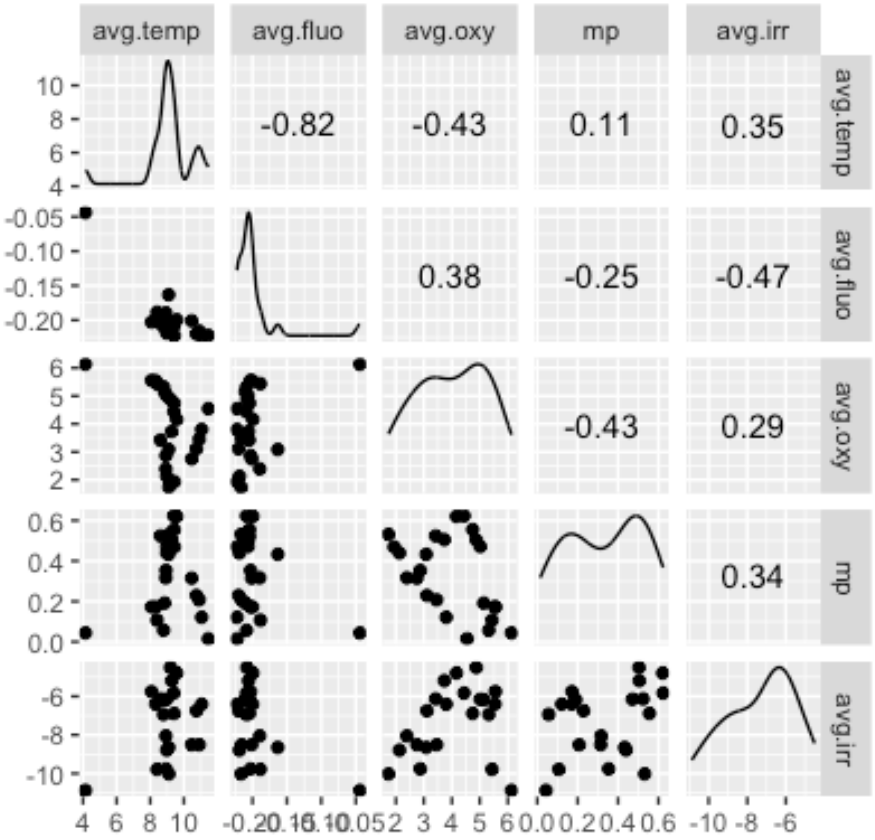

Fig. 3.4.4. Correlation matrix MP (38 kHz). Pearson's correlation coefficients between migrating proportions (mp), average oxygen 200-1000 m (avg.oxy), average fluorescence 0-200 m (avg.fluo), average temperature 200-1000 m (avg.temp), and average irradiance 0-1000 m (avg.irr) at 38 kHz.

3.5 Environmental influences on daytime WMDs

Environmental variables (oxygen, fluorescence, temperature and irradiance) were checked for correlation with daytime WMD at 18 and 38 kHz, using Pearson's correlation tests (fig. 3.5.2 and 3.5.4) and stepwise multiple linear regressions (fig. 3.5.1 and 3.5.3). I used average oxygen

200-1000 m (ml l^{-1}), average fluorescence 0-200 m (relative units, a measure of chlorophyll a fluorescence), average temperature 200-1000 m (°C), and average irradiance 0-1000 m (µmol photons/m^2/sec).

3.5.1 Stepwise multiple linear regression WMD (18 kHz)

Average irradiance had the strongest correlation with daytime WMD at 18 kHz ($\rho = 0.58$), followed by average temperature ($\rho = 0.4$), average oxygen ($\rho = 0.28$) and average fluorescence ($\rho = -0.27$).

Average irradiance (0-1000 m) appeared to explain 30,9% of the variation in daytime WMD at 18 kHz (adj. $R^2 = 0.309$). Daytime WMD appeared to increase with increasing irradiance (WMD = 16.856*(avg. irradiance) + 5.227, n = 24, $p < 0.05$).

COEFFICIENTS	ESTIMATE	STD.ERROR	T-VALUE	P-VALUE
INTERCEPT	609.389	39.324	15.497	0.000
AVG. IRRADIANCE	16.856	5.227	3.225	0.004

Fig. 3.5.1. Stepwise multiple linear regression daytime WMD (18 kHz).

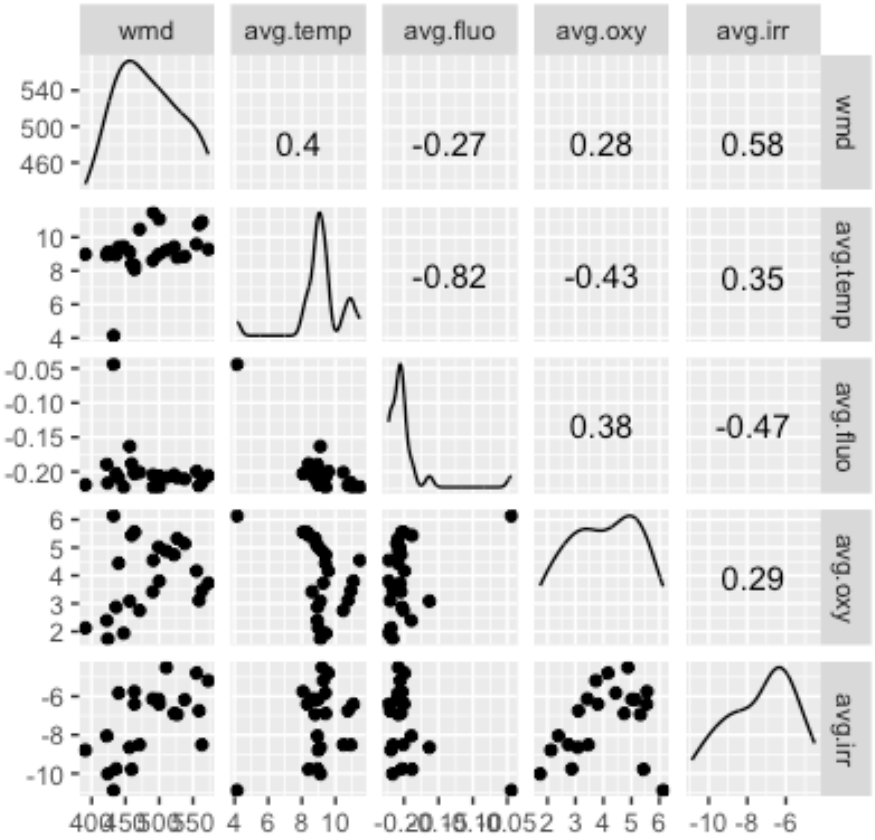

Fig. 3.5.2 Correlation matrix WMD (18 kHz). Pearson's correlation coefficients between daytime WMD (wmd), average oxygen 200-1000 m (avg.oxy), average fluorescence 0-200 m (avg.fluo), average temperature 200-1000 m (avg.temp), and average irradiance 0-1000 m (avg.irr) at 18 kHz.

3.5.2 Stepwise multiple linear regression WMD (38 kHz)

Average oxygen had the strongest correlation with daytime WMD at 38 kHz (ρ = 0.53), followed by average irradiance (ρ = 0.36), average temperature (ρ = 0.07) and average fluorescence (ρ = -0.05).

Average oxygen (200-1000 m) and average temperature (200-1000 m) appeared to explain 32.2% of the variation in daytime WMD at 38 kHz (adj. R^2 = 0.322). Daytime WMD appeared to increase with increasing oxygen and increasing temperature (WMD = 37.279*(avg. oxygen) + 17.946*(avg. temperature), n = 24). Average oxygen was statistical significant ($p < 0.05$), while average temperature was not ($p > 0.05$).

COEFFICIENTS	ESTIMATE	STD.ERROR	T-VALUE	P-VALUE
INTERCEPT	180.805	112.775	1.603	0.124
AVG. OXYGEN	37.279	10.431	3.574	0.002
AVG. TEMPERATURE	17.946	9.593	1.871	0.075

Fig. 3.5.3 Stepwise multiple linear regression WMD (38 kHz).

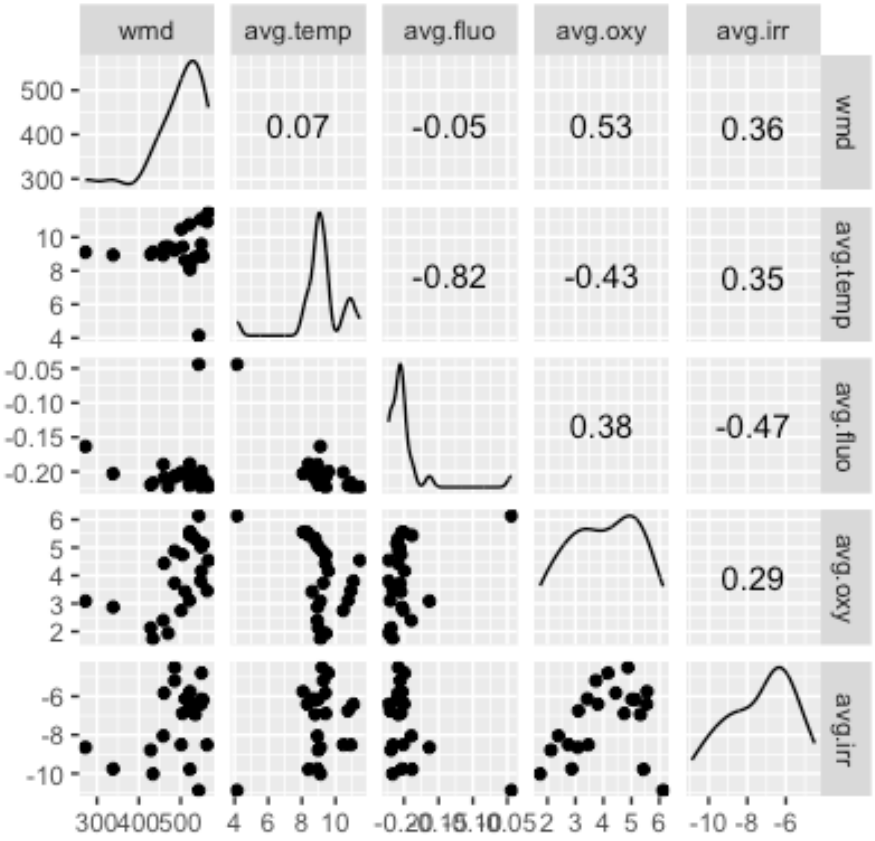

Fig. 3.5.4. Correlation matrix WMD (38 kHz). Pearson's correlation coefficients between daytime WMD (wmd), average oxygen 200-1000 m (avg.oxy), average fluorescence 0-200 m (avg.fluo), average temperature 200-1000 m (avg.temp), and average irradiance 0-1000 m (avg.irr) at 38 kHz.

4 Discussion

4.1 Environmental data

In the North Atlantic region (~38-20°N), the thermoclines and haloclines increased in depth (~200 m), the water masses were well-oxygenated throughout the water column, and the fluorescence layer decreased in depth (fig. 3.1). There was a distinct frontal zone at ~20°N, in which the thermohaloclines decreased in depth, there was a decrease in sub-surface oxygen concentrations and fluorescence increased (fig. 3.1). These water masses are part of the North Atlantic subtropical gyre, which are typically associated with deep thermoclines and well-oxygenated waters (Poole & Tomczak, 1999). The North Atlantic subtropical gyre is dominated by North Atlantic Central Water (NACW), which transitions into the South Atlantic Central Water (SACW) at ~15-20°N (Karstensen, Stramma, & Visbeck, 2008; Poole & Tomczak, 1999). The convergence of these water masses corresponds to the Cape Verde Frontal Zone (Stramma & Schott, 1999), which can be observed in the CTD profiles as a distinct shift in thermohaloclines and oxygen concentrations at ~20°N (fig. 3.1).

In the Cape Verde Frontal Zone (~15°N), the sub-surface oxygen concentrations fell below 2 ml l^{-1} , which were the lowest concentrations recorded for the study region (fig. 3.1). These low sub-surface oxygen concentrations may be associated with well-developed oxygen minimum layers (OMLs) characteristic for the eastern boundary of the North Atlantic (Karstensen et al., 2008). Although there is no agreed-upon threshold defining an OML (Karstensen et al., 2008), concentrations less than 0.1 ml l^{-1} are typically associated with the OMLs between 100-900 m in this region (Childress & Seibel, 1998). With this definition in mind, the observed low sub-surface oxygen concentrations in my data (fig. 3.1) does not describe an OML. However, since my data only reach 300 m, the possibility of an OML occurring at greater depths cannot be excluded.

The equatorial region (10°N-10°S) was characterized by high near-surface temperatures and shallow thermohaloclines, a sub-surface salinity maximum and low near-surface salinities, low sub-surface oxygen concentrations and increased fluorescence (fig. 3.1). High sea surface

temperatures (SSTs) in the equatorial region has been attributed to Tropical Surface Water (TSW), which lies above the SACW and can reach temperatures of 27°C (Stramma & Schott, 1999). The diverging westward North and South Equatorial Current (NEC and SEC) cause upwelling in the equatorial region, which ultimately drives the thermohaloclines towards the surface (Poole & Tomczak, 1999). The sub-surface salinity maximum is believed to be caused by the subduction of Salinity Maximum Water formed at the tropical/subtropical interface, while the low near-surface salinities are caused by high precipitation typical for tropical regions (Stramma & Schott, 1999). The low sub-surface oxygen concentrations found in this region seems to be part of an extensive OML between ~20°N and ~15°S (fig. 3.1). OMLs can cover vast oceanic regions (Childress & Seibel, 1998), which could provide an explanation for the observed data. The equatorial upwelling drives nutrient-rich waters towards the mixed layer, making nutrient readily available to primary producers. This is reflected in the relatively high fluorescence observed in the region (fig. 3.1).

The Brazilian shelf region (~11.5-21°S) was characterized by deep thermohaloclines, well-oxygenated waters, and a deep fluorescence layer with relatively low concentrations (fig 3.1). As previously mentioned, deep thermoclines and well-oxygenated waters are characteristic for subtropical gyres (Poole & Tomczak, 1999), and this region corresponds to the western boundary of the South Atlantic subtropical gyre. The Brazilian shelf is considered one of the most oligotrophic regions in the world (Morel et al., 2010), which may explain the deep fluorescence layer with low concentrations observed in my data (fig. 3.1). Nutrient-poor waters are associated with high water clarity, making primary production possible at greater depths (Ryabov, Rudolf, & Blasius, 2010).

In the Brazil-Malvinas Confluence region (~35-42°S), near-surface temperatures decreased, the thermohaloclines decreased in depth, the waters were well-oxygenated, the fluorescence layer decreased in depth and was characterized by the highest concentrations recorded in the study region (3.1). There was also a prominent front at ~40°S with distinctive shifts in temperature, salinity and oxygen concentrations, throughout the water column (fig. 3.1). The heterogenous water masses of the Brazil-Malvinas Confluence is result of the convergence of different water masses. The southward flowing Brazil current carries warm, saline SACW along continental margin of South America, while the Malvinas Current carries cold Subantarctic Water northward along continental margin (A. A. Bianchi et al., 1993). The merging of these opposing currents creates a thermohaline front at ~35-40°S (Brazil-Malvinas

Confluence), characterized by wide ranges in temperatures (7-18°C) and salinities (33.6-36 PSU) (Gordon, 1989).

4.2 Acoustic data

In this thesis, the acoustic backscatter was used as a proxy for relative abundance of mesopelagic micronekton. However, swimbladder resonance might invalidate my assumptions of abundance. Although resonance scatter is more prevalent at the 18 kHz frequency (Godø et al., 2009; R. Kloser et al., 2002), resonance in itself may provide information about the fish and their behaviour, and can therefore be useful when discussing species compositions (Godø et al., 2009; Pena et al., 2014). Resonance scatter also occur at the 38 kHz frequency, especially for smaller individuals (< 4 cm) in deep layers, and for fishes with regressed swimbladders (P. C. Davison et al., 2015; Rudy J. Kloser, Ryan, Keith, & Gershwin, 2016).

4.2.1 Vertical distributions (18 and 38 kHz)

The mean acoustic backscatter (s_A) recorded at 18 and 38 kHz showed clear day and night effects on the vertical distribution, with increased scatter in the epipelagic (0-200 m) at night and increased scatter in the mesopelagic (200-1000 m) at day (fig. 3.2.1). This is a common feature of the world ocean and is attributed to mesopelagic organisms exhibiting diel vertical migration (DVM) behaviour (T. A. Klevjer et al., 2016; Sutton, 2013).

The 38 kHz distribution displayed higher values of mean acoustic backscatter (s_A) in the mesopelagic at both daytime and night-time compared with the 18 kHz distribution (fig. 3.2.1). This is also reflected in the daytime weighted mean depths (WMD), which was deeper at the 38 kHz distribution than the 18 kHz distribution (table. 3.2.1). A study Pena et al. (2020) using multiple frequencies to detect scattering layers in the North Atlantic, found that non-migrating layers in the mesopelagic had a higher response at 38 kHz. This suggest that the increased abundance observed in the mesopelagic layer at 38 kHz (fig 3.2.1), may be attributed to the presence of non-migratory species remaining in the mesopelagic at both daytime and night-time. Several species of the genus Cyclothone are non-migratory (Olivar et al., 2017) and has

a frequency response matching that of 38 kHz (Pena et al., 2014). Cyclothone spp. is also one considered the most abundant vertebrate in the world, typically dominating lower mesopelagic layers (Olivar et al., 2012; Ross, Quattrini, Roa-Varón, & McClain, 2010). Although species identification is usually achieved by ground-truthing (trawl data) and/or multi-frequency identification (R. Kloser et al., 2002), the possibility of Cyclothone spp. being one of the main contributors to the increased scatter observed in the mesopelagic at 38 kHz, can't be ruled out.

Furthermore, Pena et al. (2020) found that migrating layers in the mesopelagic had a higher frequency response at 18 kHz (down to ~600 m). This is reflected in my results, as the 18 kHz distribution displayed decreased scatter in the mesopelagic at night (fig. 3.2.1) and higher migrating proportions (table. 3.2.1). Increased frequency response at 18 kHz is consistent with the characteristics of Myctophidae ('Lanternfish') (Godø et al., 2009). Myctophids have swimbladders which undergo changes in frequency response as they migrate towards the epipelagic on a daily cycle, making them resonant at this frequency (Godø et al., 2009). Myctophids are also one of the most abundant families found in mesopelagic layers (R. Kloser et al., 2002; Olivar et al., 2017)

4.2.2 Vertical distributions between regions (18 and 38 kHz)

The NE Atlantic region (~46-36°N) was characterized by relatively low acoustic backscatter (s_A) on both frequencies (fig. 3.2.2 and fig. 3.2.3), which may reflect the low mesopelagic biomass estimates in this region (Gjøsæter & Kawaguchi, 1980). The presence of two shallow daytime scattering layers at the 18 kHz distribution (~200 m and ~325) may suggest that the species composition differ between the layers. Godø et al. (2009) on DVM behaviour and swimbladder resonance in the North Atlantic, found a migrating shallow layer (~200 m) dominated by Pearlsides (*Maurolicus muelleri*), and a migrating deeper layer (~400-500 m) dominated by Myctophids. The night-time distribution recorded at 38 kHz showed a prominent non-migratory deep layer and very limited acoustic scatter in the epipelagic (fig. 3.2.3), contributing do the deep daytime WMD observed in this region (table 3.2.3). This indicates that the region is dominated by non-migrant species (e.g. Cyclothone spp. or non-migrating myctophids). This was also demonstrated by the low MP in the region, which was 14% at the 18 kHz distribution and 2% at the 38 kHz distribution (table. 3.2.2). T. A. Klevjer et al. (2016)

found that MP increased with decreasing oxygen, decreasing turbidity and increasing SST temperature, and that daytime WMD increased with increasing oxygen and decreasing fluorescence. My environmental data shows that the NE Atlantic region is characterized by well-oxygenated waters and low near-surface temperature (fig. 3.1), which might contribute to the low MPs and deep daytime WMDs in the region (table. 3.2.2 and 3.2.3).

The Cape Verde frontal region (17-11°N) displayed distinctive night-time layers in the epipelagic at both frequencies, characterized by relatively high scatter (fig. 3.2.2 and fig. 3.2.3). The MP was the highest recorded between regions, reaching 69,4% at 18 kHz and 50,5% at 38 kHz, while daytime WMDs were relatively shallow compared to other regions (table 3.2.2 and table 3.2.3). My environmental data shows that the Cape Verde frontal region (17-11°N) had very low sub-surface oxygen concentrations, high near-surface temperatures, and relatively high fluorescence (fig. 3.1), which all have been associated with high MPs and shallow WMDs (Daniele Bianchi et al., 2013; T. A. Klevjer et al., 2016).

The equatorial region (~10°N-10°S) displayed distinctive night-time layers in the epipelagic at both frequencies (fig. 3.2.2 and 3.2.3), which was reflected by the relatively high MPs estimated for the region (table 3.2.2 and table 3.2.3). The daytime WMDs were shallow at both frequencies, although more so at 38 kHz (WMD = 386) (table 3.2.3). My environmental data shows that sub-surface oxygen concentrations were low, near-surface temperatures were high and fluorescence was increased in this regions (fig. 3.1) which could cause high MPs and shallow daytime WMDs (Daniele Bianchi et al., 2013; T. A. Klevjer et al., 2016).

The Brazilian shelf region (~11.5-21°S) was characterized by several epipelagic night-time layers at both frequencies (18 and 38 kHz), stretching from the sea surface towards ~250 m (fig. 3.2.2 and fig. 3.2.3). This may be attributed to a combination of a deep fluorescence maximum layer and high species diversity in the region. The fluorescence maximum observed at the Brazilian shelf was the deepest recorded in the study region, reaching ~200 m (fig. 3.1). This indicates that available food resources are distributed within a greater depth range (deeper mixed layer), making ascent all the way toward the sea surface unnecessary for some species (Andersen & Nival, 1991). Furthermore, oligotrophic regions, i.e. the Brazilian shelf (see Morel et al. (2010)), have been associated with higher species richness compared to eutrophic regions (Andersen, Sardou, & Gasser, 1997). Oligotrophic regions are old and stable ecosystems which have enabled the evolution of similar species niches, and as a consequence,

competition for limited resources such as food and space is common (Hopkins & Sutton, 1998). However, feeding at different migration depths minimize competition between species and populations, and consequently maintains high species diversity (Hopkins & Sutton, 1998). This may explain the occurrence of several epipelagic scattering layers at night in this region (fig. 3.2.2 and fig. 3.2.3). The 18 kHz distribution displayed several deep daytime scattering layers between ~375-875 m (fig. 3.2.2), reflecting the deep daytime WMD (505 m) estimated at this frequency (table 3.2.2). This may be attributed to the high water clarity characteristic for the region. Low productivity is typically associated with clear water masses, in which light penetrates deeper into the water column. Light is a well-known proximate cue for DVM, and high water clarity (i.e. deeper light penetration) have been associated with deeper daytime distributions (Onsrud & Kaartvedt, 1998). The migrating proportions were relatively high at 38 kHz (58.9%), which might be associated with the low turbidity (high water clarity) characteristic for the region, and high near-surface temperatures (fig. 3.1) (T. A. Klevjer et al., 2016). My environmental data shows that the Brazilian shelf region (~11.5-21°S) was also characterized by well-oxygenated waters and low fluorescence (fig. 3.1), which have been associated with deep WMDs (Daniele Bianchi et al., 2013; T. A. Klevjer et al., 2016).

The Brazil-Malvinas Confluence (~35-42°S) distribution recorded at 18 kHz was characterized by a relative high abundance in between the two night-time scattering layers at ~80 m and ~375 m (fig. 3.2.2). Similar to the epipelagic distribution in the Brazilian shelf region, the extensive depth range of this night-time distribution may be attributed to species composition. A study by Figueroa, DíAz De Astarloa, and Martos (1998) on mesopelagic fish distribution in the Brazil-Malvinas Confluence, found that the species composition was characterized by a mix of sub-Antarctic species of the Malvinas current, tropical-subtropical species of the Brazil current and sub-Antarctic-subtropical convergence species. Although the species richness of this eutrophic region might not be that of the oligotrophic Brazilian shelf (Andersen et al., 1997), the merging of species of varying biogeographical origins might reflect on the wide depth range of the epipelagic night-time layer (fig. 3.2.2 and fig. 3.2.3). The 38 kHz distribution displayed a distinct non-migratory night-time layer, reflected in the relatively low MPs and deep daytime WMDs estimated in this region (table. 3.2.2 and table 3.2.3). My environmental data shows that this region was characterized by higher oxygen concentrations and lower near-surface temperatures (fig. 3.1) which have been associated with low MPs (Daniele Bianchi et al., 2013; T. A. Klevjer et al., 2016)

4.3 Latitudinal distribution

The latitudinal distribution displayed high variability between frequencies (18 and 38 kHz) in the North Atlantic (46-10°N) and in the in the Brazil-Malvinas Confluence region (35-42°S) (fig. 3.3). Both these regions are characterized by distinct non-migratory deep layers recorded at 38 kHz (fig. 3.2.3), which may account for the relatively high acoustic scatter at this frequency (fig. 3.3). Non-migratory deep layers are often associated with Cyclothone spp., which are highly abundant in the mesopelagic and resonates at 38 kHz (Pena et al., 2014). However, the assumption of abundance should be made with care due to swimbladder resonance at depth (P. C. Davison et al., 2015). The relatively low acoustic scatter recorded at 18 kHz in the North East Atlantic (46-35°N) may be due to low abundance or non-resonant fish. According to the works of Gjøsæter and Kawaguchi (1980), biomass estimates in the North East Atlantic are relatively low compared to other regions in the Atlantic Ocean.

The low variability between frequencies in the equatorial region (10°N-10°S) and the Brazilian shelf (11,5-21°S) may be attributed to the high proportion of migrants relative to the non-migratory layers at 38 kHz (fig. 3.2.3, table 3.2.3). The higher proportion of migrants in this region (table. 3.2.2) will also contribute to the increased scatter at 18 kHz, seeing as a lot of migratory myctophids resonate at this frequency (Pena et al., 2014). Furthermore, the Brazilian shelf (11,5-21°S) has been characterized as an oligotrophic region (Morel et al., 2010) with low biomass (Olivar et al., 2017), which would explain the low acoustic scatter on both frequencies in this region (fig. 3.3).

4.4 Environmental influences on migrating proportions

The proportion of migrants (MP) recorded at 18 kHz and 38 kHz were both inversely correlated with average oxygen (200-1000 m) (fig. 3.4.2, fig. 3.4.3). A similar relationship between MP and mid-water oxygen concentrations has been described in T. A. Klevjer et al. (2016), although their study did not include acoustic backscatter recorded at 18 kHz.

Mesopelagic species have developed several strategies to supress metabolic rates, which enables them to tolerate hypoxic conditions at daytime (Brad A Seibel, 2011). Some of these

strategies include anaerobic metabolism, reducing locomotor activity and adaptations for oxygen extraction and storage (Childress & Seibel, 1998; Brad A Seibel, 2011). However, most mesopelagic species are not able to permanently live in well-developed oxygen minima layers (<0.15 ml l^{-1}) and have to migrate towards shallower and more oxygenated waters at night (Childress & Seibel, 1998).

The results from the stepwise multiple regression on MP at 38 kHz showed that mean oxygen (200-100 m) and mean irradiance (0-1000 m) appear to explain 32.7% of the variation (adj. R^2 = 0.327, $p < 0.05$, n = 24), in which MP appear to increase with decreasing oxygen and increasing irradiance (fig. 3.4.3). An increase in MP with increasing irradiance is comparable with the results attained by T. A. Klevjer et al. (2016) where they found that MP increased with decreasing turbidity (effectively a measure of light scattering).

4.5 Environmental influences on daytime WMDs

The results from the stepwise linear regression on daytime WMD at 18 kHz show that average irradiance (0-1000 m) appear to explain 30,9% of the variation (adj. R^2 = 0.309, n = 24, $p < 0.05$), in which daytime WMD appear to increase with increasing irradiance (fig. 3.5.1).

The association between light penetration and daytime scattering layers has been established for a long time (Dickson, 1972; Roe, 1983). Mesopelagic organisms have been found to occupy a so called light comfort zone (LCZ), in which they avoid too strong and too low light levels (Dupont, Klevjer, Kaartvedt, & Aksnesa, 2009). Staying at depths with high light intensities would increase feeding rates, but also increase the risk of mortality through predation (Rosland & Giske, 1994). The optimal depth at which mesopelagic organisms position themselves may therefore represent a compromise between feeding opportunity and risk of predation (Rosland & Giske, 1994). A recent study that also used direct underwater irradiance measurements to address the role of light penetration at mesopelagic depths (Aksnes et al., 2017), found that the global variability in daytime scattering layers were governed by variation in light penetration.

The results from the stepwise linear regression on daytime WMD at 38 kHz, show that average oxygen (200-1000 m) and average temperature (200-1000 m) appear to explain 32.2% of the

variation (adj. $R^2 = 0.322$), in which daytime WMD appear to increase with increasing oxygen and increasing temperature (fig. 3.5.3). Although, the estimate of average temperature was not significant ($p > 0.05$).

The association between greater daytime migration depths and higher oxygen concentrations have been found by several studies (Daniele Bianchi et al., 2013; Thor Aleksander Klevjer et al., 2016; Netburn & Koslow, 2015). The correlation between deep daytime scattering layers and higher subsurface oxygen concentrations may be attributed to predator avoidance, in which low-oxygenated waters may provide a refuge from visual predators with higher oxygen demands (Brad A Seibel, 2011). Entering low-oxygenated water may also be an adaptive strategy to save energy through metabolic suppression (Brad A. Seibel et al., 2014).

Although the correlation between greater daytime migration depths and higher oxygen concentrations appear to be strong, Aksnes et al. (2017) argues that the overall association between DSL and oxygen is due to a negative relationship between light attenuation and dissolved oxygen, in which light penetration decrease in hypoxic waters.

Although the temperature variables was not significant in my model (fig. 3.5.3), it appeared to explain a larger fraction of the variance than oxygen alone. Increased daytime migration depths have been found to correlate with increasing temperatures (Cade & Benoit-Bird, 2015). The relationship between temperature and daytime WMDs may be attributed to the conservation of energy by scattering layer organism residing in cooler, deeper waters (Childress & Seibel, 1998).

Average irradiance appear to have the strongest correlation with daytime WMD's at the 18 kHz frequency (fig. 3.5.2), while oxygen appear to have the strongest correlation with daytime WMD's at the 38 kHz frequency (fig. 3.5.4). The fact that the predictors of daytime WMDs varies between frequencies, may be attributed to the importance of different environmental factors at varying depths. My results show that daytime WMDs are shallower at the 18 kHz distribution (472 m) compared to the 38 kHz distribution (494 m) (fig. 3.2.1). Interestingly, Netburn and Koslow (2015) found that upper daytime scattering layer boundary depths correlated best with irradiance and dissolved oxygen, while bottom daytime scattering layer boundary depths correlated most strongly with dissolved oxygen. The study hypothesized that daytime scattering layers would increase with increasing oxygen concentrations at the bottom

layer due its proximity to hypoxic waters (Netburn & Koslow, 2015). Although the study only applied acoustic data recorded at 38 kHz, this apparent change in predictors at the upper and lower boundaries of the daytime scattering layers may explain why different predictors were important between frequencies in my model.

References

Aksnes, D. L., Rostad, A., Kaartvedt, S., Martinez, U., Duarte, C. M., & Irigoien, X. (2017). Light penetration structures the deep acoustic scattering layers in the global ocean. *Science Advances, 3*(5), 5. doi:10.1126/sciadv.1602468

Andersen, V., & Nival, P. (1991). A model of the diel vertical migration of zooplankton based on euphausiids. *Journal of Marine Research, 49*(1), 153-175. doi:10.1357/002224091784968594

Andersen, V., Sardou, J., & Gasser, B. (1997). Macroplankton and micronekton in the northeast tropical Atlantic: abundance, community composition and vertical distribution in relation to different trophic environments. *Deep Sea Research Part I: Oceanographic Research Papers, 44*(2), 193-222. doi:10.1016/s0967-0637(96)00109-4

Bianchi, D., Galbraith, E. D., Carozza, D. A., Mislan, K., & Stock, C. A. (2013). Intensification of open-ocean oxygen depletion by vertically migrating animals. *Nature Geoscience, 6*(7), 545.

Bianchi, D., & Mislan, K. A. S. (2016). Global patterns of diel vertical migration times and velocities from acoustic data. *Limnology and Oceanography, 61*(1), 353-364. doi:10.1002/lno.10219

Bianchi, A. A., Giulivi, C. F., & Piola, A. R. (1993). Mixing in the Brazil-Malvinas confluence. *Deep Sea Research Part I: Oceanographic Research Papers, 40*(7), 1345-1358. doi:10.1016/0967-0637(93)90115-j

Bollens, S. M., Rollwagen-Bollens, G., Quenette, J. A., & Bochdansky, A. B. (2010). Cascading migrations and implications for vertical fluxes in pelagic ecosystems. *Journal of Plankton Research, 33*(3), 349-355.

Cade, D. E., & Benoit-Bird, K. J. (2015). Depths, migration rates and environmental associations of acoustic scattering layers in the Gulf of California. *Deep-Sea Research Part I-Oceanographic Research Papers, 102*, 78-89. doi:10.1016/j.dsr.2015.05.001

Childress, J. J., & Seibel, B. A. (1998). Life at stable low oxygen levels: Adaptations of animals to oceanic oxygen minimum layers. *Journal of Experimental Biology, 201*(8), 1223-1232. Retrieved from <Go to ISI>://WOS:000073772900016

Christiansen, S., Klevjer, T. A., Røstad, A., Aksnes, D. L., & Kaartvedt, S. (2021). Flexible behaviour in a mesopelagic fish (Maurolicus muelleri). *ICES Journal of Marine Science*. doi:10.1093/icesjms/fsab075

Davison, P. (2011). The specific gravity of mesopelagic fish from the northeastern Pacific Ocean and its implications for acoustic backscatter. *ICES Journal of Marine Science, 68*(10), 2064-2074. doi:10.1093/icesjms/fsr140

Davison, P., Checkley Jr, D., Koslow, J., & Barlow, J. (2013). Carbon export mediated by mesopelagic fishes in the northeast Pacific Ocean. *Progress in Oceanography, 116*, 14-30.

Davison, P. C., Koslow, J. A., & Kloser, R. J. (2015). Acoustic biomass estimation of mesopelagic fish: backscattering from individuals, populations, and communities. *ICES Journal of Marine Science, 72*(5), 1413-1424.

Dickson, R. (1972). On the relationship between ocean transparency and the depth of sonic scattering layers in the North Atlantic. *ICES Journal of Marine Science, 34*(3), 416-422.

Dupont, N., Klevjer, T. A., Kaartvedt, S., & Aksnesa, D. L. (2009). Diel vertical migration of the deep-water jellyfish Periphylla periphylla simulated as individual responses to absolute light intensity. *Limnology and Oceanography, 54*(5), 1765-1775. doi:10.4319/lo.2009.54.5.1765

Escobar-Flores, P. C., O'Driscoll, R. L., & Montgomery, J. C. (2018). Predicting distribution and relative abundance of mid-trophic level organisms using oceanographic parameters and acoustic backscatter. *Marine Ecology Progress Series, 592*, 37-56. doi:10.3354/meps12519

Figueroa, D. E., DíAz De Astarloa, J. M., & Martos, P. (1998). Mesopelagic fish distribution in the southwest Atlantic in relation to water masses. *Deep Sea Research Part I: Oceanographic Research Papers, 45*(2-3), 317-332. doi:10.1016/s0967-0637(97)00076-9

Gilly, W. F., Beman, J. M., Litvin, S. Y., & Robison, B. H. (2013). Oceanographic and biological effects of shoaling of the oxygen minimum zone. *Annual review of marine science, 5*, 393-420.

Gjøsæter, J., & Kawaguchi, K. (1980). *A review of the world resources of mesopelagic fish*: Food & Agriculture Org.

Godo, O. R., Patel, R., & Pedersen, G. (2009). Diel migration and swimbladder resonance of small fish: some implications for analyses of multifrequency echo data. *ICES Journal of Marine Science, 66*(6), 1143-1148. doi:10.1093/icesjms/fsp098

Godø, O. R., Patel, R., & Pedersen, G. (2009). Diel migration and swimbladder resonance of small fish: some implications for analyses of multifrequency echo data. *ICES Journal of Marine Science, 66*(6), 1143-1148.

Gordon, A. L. (1989). Brazil-Malvinas Confluence–1984. *Deep Sea Research Part A. Oceanographic Research Papers, 36*(3), 359-384. doi:10.1016/0198-0149(89)90042-3

Handegard, N. O., Buisson, L. D., Brehmer, P., Chalmers, S. J., De Robertis, A., Huse, G., . . . Godø, O. R. (2013). Towards an acoustic-based coupled observation and modelling system for monitoring and predicting ecosystem dynamics of the open ocean. *Fish and Fisheries, 14*(4), 605-615. doi:10.1111/j.1467-2979.2012.00480.x

Hays, G. C. (2003). A review of the adaptive significance and ecosystem consequences of zooplankton diel vertical migrations. In *Migrations and dispersal of marine organisms* (pp. 163-170): Springer.

Hopkins, T. L., & Sutton, T. T. (1998). Midwater fishes and shrimps as competitors and resource partitioning in low latitude oligotrophic ecosystems. *Marine Ecology Progress Series, 164*, 37-45. doi:10.3354/meps164037

Irigoien, X., Klevjer, T. A., Røstad, A., Martinez, U., Boyra, G., Acuña, J., . . . Hernandez-Leon, S. (2014). Large mesopelagic fishes biomass and trophic efficiency in the open ocean. *Nature communications, 5*, 3271.

Karstensen, J., Stramma, L., & Visbeck, M. (2008). Oxygen minimum zones in the eastern tropical Atlantic and Pacific oceans. *Progress in Oceanography, 77*(4), 331-350. doi:10.1016/j.pocean.2007.05.009

Kase, R. H., Zenk, W., Sanford, T. B., & Hiller, W. (1985). CURRENTS, FRONTS AND EDDY FLUXES IN THE CANARY BASIN. *Progress in Oceanography, 14*(1-4), 231-257. doi:10.1016/0079-6611(85)90013-8

Klevjer, T., Melle, W., Knutsen, T., Strand, E., Korneliussen, R., Dupont, N., . . . Wiebe, P. H. (2020). Micronekton biomass distribution, improved estimates across four north Atlantic basins. *Deep-Sea Research Part Ii-Topical Studies in Oceanography, 180*. doi:10.1016/j.dsr2.2019.104691

Klevjer, T. A., Irigoien, X., Røstad, A., Fraile-Nuez, E., Benítez-Barrios, V. M., & Kaartvedt, S. (2016). Large scale patterns in vertical distribution and behaviour of mesopelagic scattering layers. *Scientific reports, 6*(1), 19873. doi:10.1038/srep19873

Klevjer, T. A., Irigoien, X., Røstad, A., Fraile-Nuez, E., Benítez-Barrios, V. M., & Kaartvedt, S. (2016). Large scale patterns in vertical distribution and behaviour of mesopelagic scattering layers. *Scientific reports, 6*, 19873. Retrieved from https://www.ncbi.nlm.nih.gov/pmc/articles/PMC4728495/pdf/srep19873.pdf

Kloser, R., Ryan, T., Sakov, P., Williams, A., & Koslow, J. (2002). Species identification in deep water using multiple acoustic frequencies. *Canadian Journal of Fisheries and Aquatic Sciences, 59*(6), 1065-1077.

Kloser, R. J., Ryan, T. E., Keith, G., & Gershwin, L. (2016). Deep-scattering layer, gas-bladder density, and size estimates using a two-frequency acoustic and optical

probe. *ICES Journal of Marine Science, 73*(8), 2037-2048. doi:10.1093/icesjms/fsv257

Kloser, R. J., Ryan, T. E., Young, J. W., & Lewis, M. E. (2009). Acoustic observations of micronekton fish on the scale of an ocean basin: potential and challenges. *ICES Journal of Marine Science, 66*(6), 998-1006.

Koslow, J. A., Goericke, R., Lara-Lopez, A., & Watson, W. (2011). Impact of declining intermediate-water oxygen on deepwater fishes in the California Current. *Marine Ecology Progress Series, 436*, 207-218.

Koslow, J. A., Kloser, R. J., & Williams, A. (1997). Pelagic biomass and community structure over the mid-continental slope off southeastern Australia based upon acoustic and midwater trawl sampling. *Marine Ecology Progress Series, 146*, 21-35.

Kaartvedt, S., Titelman, J., Røstad, A., & Klevjer, T. A. (2011). Beyond the average: Diverse individual migration patterns in a population of mesopelagic jellyfish. *Limnology and Oceanography, 56*(6), 2189-2199.

Lehodey, P., Murtugudde, R., & Senina, I. (2010). Bridging the gap from ocean models to population dynamics of large marine predators: A model of mid-trophic functional groups. *Progress in Oceanography, 84*(1-2), 69-84. doi:10.1016/j.pocean.2009.09.008

Maillard, C., & Kase, R. (1989). THE NEAR-SURFACE FLOW IN THE SUB-TROPICAL GYRE SOUTH OF THE AZORES. *Journal of Geophysical Research-Oceans, 94*(C11), 16133-16140. doi:10.1029/JC094iC11p16133

Morel, A., Claustre, H., & Gentili, B. (2010). The most oligotrophic subtropical zones of the global ocean: similarities and differences in terms of chlorophyll and yellow substance. *Biogeosciences, 7*(10), 3139-3151. doi:10.5194/bg-7-3139-2010

Netburn, A. N., & Koslow, J. A. (2015). Dissolved oxygen as a constraint on daytime deep scattering layer depth in the southern California current ecosystem. *Deep Sea Research Part I: Oceanographic Research Papers, 104*, 149-158.

New, A. L., Jia, Y., Coulibaly, M., & Dengg, J. (2001). On the role of the Azores Current in the ventilation of the North Atlantic Ocean. *Progress in Oceanography, 48*(2-3), 163-194. doi:10.1016/s0079-6611(01)00004-0

Olivar, M. P., Bernal, A., Molí, B., Peña, M., Balbín, R., Castellón, A., . . . Massutí, E. (2012). Vertical distribution, diversity and assemblages of mesopelagic fishes in the western Mediterranean. *Deep Sea Research Part I: Oceanographic Research Papers, 62*, 53-69. doi:10.1016/j.dsr.2011.12.014

Olivar, M. P., Hulley, P. A., Castellon, A., Emelianov, M., Lopez, C., Tuset, V. M., . . . Moli, B. (2017). Mesopelagic fishes across the tropical and equatorial Atlantic:

Biogeographical and vertical patterns. *Progress in Oceanography, 151*, 116-137. doi:10.1016/j.pocean.2016.12.001

Onsrud, M., & Kaartvedt, S. (1998). Diel vertical migration of the krill Meganyctiphanes norvegica in relation to physical environment, food and predators. *Marine Ecology Progress Series, 171*, 209-219. doi:10.3354/meps171209

Pearre, S. (2003). Eat and run? The hunger/satiation hypothesis in vertical migration: history, evidence and consequences. *Biological Reviews, 78*(1), 1-79.

Pena, M., Cabrera-Gamez, J., & Dominguez-Brito, A. C. (2020). Multi-frequency and light-avoiding characteristics of deep acoustic layers in the North Atlantic. *Marine Environmental Research, 154*. doi:10.1016/j.marenvres.2019.104842

Pena, M., Olivar, M. P., Balbin, R., Lopez-Jurado, J. L., Iglesias, M., & Miquel, J. (2014). Acoustic detection of mesopelagic fishes in scattering layers of the Balearic Sea (western Mediterranean). *Canadian Journal of Fisheries and Aquatic Sciences, 71*(8), 1186-1197. doi:10.1139/cjfas-2013-0331

Penta, B., Lee, Z., Kudela, R. M., Palacios, S. L., Gray, D. J., Jolliff, J. K., & Shulman, I. G. (2008). An underwater light attenuation scheme for marine ecosystem models. *Optics Express, 16*(21), 16581-16591. doi:10.1364/oe.16.016581

Poole, R., & Tomczak, M. (1999). Optimum multiparameter analysis of the water mass structure in the Atlantic Ocean thermocline. *Deep Sea Research Part I: Oceanographic Research Papers, 46*(11), 1895-1921. doi:10.1016/s0967-0637(99)00025-4

Roe, H. (1983). Vertical distributions of euphausiids and fish in relation to light intensity in the Northeastern Atlantic. *Marine Biology, 77*(3), 287-298.

Rosland, R., & Giske, J. (1994). A dynamic optimization model of the diel vertical distribution of a pelagic planktivorous fish. *Progress in Oceanography, 34*(1), 1-43.

Ross, S. W., Quattrini, A. M., Roa-Varón, A. Y., & McClain, J. P. (2010). Species composition and distributions of mesopelagic fishes over the slope of the north-central Gulf of Mexico. *Deep Sea Research Part II: Topical Studies in Oceanography, 57*(21-23), 1926-1956. doi:10.1016/j.dsr2.2010.05.008

Ryabov, A. B., Rudolf, L., & Blasius, B. (2010). Vertical distribution and composition of phytoplankton under the influence of an upper mixed layer. *Journal of Theoretical Biology, 263*(1), 120-133. doi:10.1016/j.jtbi.2009.10.034

Seibel, B. A. (2011). Critical oxygen levels and metabolic suppression in oceanic oxygen minimum zones. *Journal of Experimental Biology, 214*(2), 326-336.

Seibel, B. A., Häfker, N. S., Trübenbach, K., Zhang, J., Tessier, S. N., Pörtner, H.-O., . . . Storey, K. B. (2014). Metabolic suppression during protracted exposure to

hypoxia in the jumbo squid, Dosidicus gigas, living in an oxygen minimum zone. *Journal of Experimental Biology, 217*(14), 2555-2568. doi:10.1242/jeb.100487

St. John, M. A., Borja, A., Chust, G., Heath, M., Grigorov, I., Mariani, P., . . . Santos, R. S. (2016). A Dark Hole in Our Understanding of Marine Ecosystems and Their Services: Perspectives from the Mesopelagic Community. *Frontiers in Marine Science, 3*(31). doi:10.3389/fmars.2016.00031

Staby, A., & Aksnes, D. L. (2011). Follow the light—diurnal and seasonal variations in vertical distribution of the mesopelagic fish Maurolicus muelleri. *Marine Ecology Progress Series, 422*, 265-273.

Stramma, L., & Schott, F. (1999). The mean flow field of the tropical Atlantic Ocean. *Deep Sea Research Part II: Topical Studies in Oceanography, 46*(1-2), 279-303. doi:10.1016/s0967-0645(98)00109-x

Stramma, L., Steele, J., Thorpe, S., & Turekian, K. (2001). Current systems in the Atlantic Ocean. *Ocean Currents*, 3-12.

Sutton, T. (2013). Vertical ecology of the pelagic ocean: classical patterns and new perspectives. *Journal of Fish Biology, 83*(6), 1508-1527.

Warrant, E. J., & Locket, N. A. (2004). Vision in the deep sea. *Biological Reviews, 79*(3), 671-712.